Joint 48th IEEE Conference on Decision and Control and
28th Chinese Control Conference
Shanghai, P.R. China, December 16-18, 2009

A Multiplay Model for Rate-Independent and Rate-Dependent Hysteresis with Nonlocal Memory

Bojana Drincic and Dennis S. Bernstein

Abstract— **We consider the multiplay model for hysteresis with nonlocal memory. This model consists of N mass/spring/dashpot with deadzone elements. The hysteresis map of the multiplay model is completely determined by the stiffness coefficients and widths of the gaps of the mass/spring/dashpot with deadzone elements. This multiplay model can be used to model a hysteretic system with a hysteresis map possessing the symmetry of the cyclic rotation group C_2. Parameters of the multiplay model can be determined based on the slope of the sampled hysteresis map. Once the multiplay model is determined, its inverse can be analytically computed.**

I. INTRODUCTION

Hysteresis is manifested as a non-vanishing input-output loop for inputs at asymptotically low frequency. This phenomenon arises in nonlinear systems with multiple attracting equilibria. In the limit of dc operation, the output is attracted to different equilibria depending on the direction of the input, which results in a nontrivial input-output loop called the *hysteresis map* [1, 2].

Several types of models can capture hysteretic behavior. Duhem and nonlinear feedback models are finite dimensional. Differential equations of Duhem models involve derivatives of the input [3, 4]. Various types of Duhem models including Maxwell-slip are described in [5]. Nonlinear feedback models consist of a linear system with a feedback nonlinearity [6]. Preisach and Prandtl-Ishlinskii models, which are infinite dimensional, consist of an infinite number of hysterons or unitary hysteresis operators, which are turned on or off depending on the current direction of the input [7]. The Prandtl-Ishlinskii model, which is a special type of the Preisach model, utilizes the play operators weighted by a density function [4, 8–10].

If the shape of the hysteresis map changes with the frequency of the input, the model is said to be *rate dependent*. If the shape of the hysteresis map is identical for all frequencies of the input, the model is *rate independent*. Nonlinear feedback models are rate dependent [6], Preisach and Prandtl-Ishlinskii models are rate independent [10] and can be extended to rate dependent [11], and Duhem models can be either rate independent or rate dependent [5].

Some hysteresis models have nonlocal memory, that is, the shape and position of the hysteresis map depend on the initial conditions. Nonlocal memory is manifested as the existence of congruent minor loops corresponding to input reversals [5, 12]. Infinite dimensional Preisach and Prandtl-Ishlinskii models capture this property [7, 8]. However, we introduce a finite-dimensional nonlinear feedback model with nonlocal memory called the multiplay model. This rate-dependent model is equivalent to the Maxwell-slip model in the limit of DC operation and can be analytically inverted which makes it suitable for real-time applications.

In this paper, we first demonstrate that the multiplay model is a rate-dependent model with nonlocal memory. Second, we make the connection between the Maxwell-slip model and the nonlinear feedback model. Third, we extend the Maxwell-slip model by introducing negative stiffness coefficients, which give greater flexibility to the shape of the hysteresis map. Next, we present a method for fitting the nonlinear feedback model to hysteresis maps possessing the symmetry of the cyclic rotation group C_2. Finally, we introduce a simple algorithm for analytically inverting a given hysteresis map.

II. MULTIPLAY

Consider the mass/spring/dashpot system with deadzone shown in Fig. 1. This system consists of a mass with mass m, a spring with stiffness k, a dashpot with damping coefficient c, and a deadzone of width 2Δ. The input u is the position of the right end of the spring, and the output x is the position of the mass. The system is modeled by the differential equation

$$m\ddot{x}(t) + c\dot{x}(t) + kd_{2\Delta}\big(x(t) - u(t)\big) = 0, \quad x(0) = x_0, \quad t \geq 0, \tag{1}$$

where

$$d_{2\Delta}(v) \triangleq \begin{cases} v + \Delta, & v \geq \Delta, \\ 0, & |v| < \Delta, \\ v - \Delta, & v \leq -\Delta \end{cases} \tag{2}$$

is the deadzone function with width $2\Delta \geq 0$.

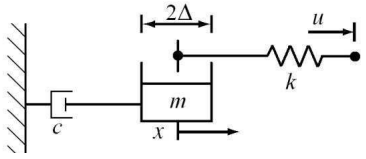

Fig. 1. Mass/spring/dashpot system with deadzone. The input u is the position of the right end of the spring, and output x is the position of the mass. The system is modeled by (1) and the deadzone is modeled by (2).

This work was supported by the NSF grant CMMI 0758363.

B. Drincic is a graduate student at the Aerospace Engineering Department, University of Michigan bojanad@umich.edu

D. S. Bernstein is with Faculty of Aerospace Engineering, University of Michigan, 1320 Beal Ave, Ann Arbor, MI 48105 dsbaero@umich.edu

The mass/spring/dashpot system with deadzone in Fig. 1 can be represented as in Fig. 2, where the mass with deadzone is replaced by the play operator discussed in [13]. In the present paper we work directly with the model (1) rather than the play operator.

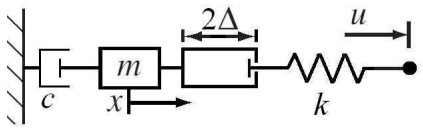

Fig. 2. Play operator representation of the mass/spring/dashpot with deadzone system. The deadzone is replaced by the play operator of width 2Δ.

Next, we define multiplay as the parallel connection of N mass/spring/dashpot systems with deadzone shown in Fig. 3. The multiplay system has N masses, N play operators with widths $2\Delta_i$, N springs with stiffness coefficients k_i, and N dashpots with damping coefficients c_i. The mass/spring/dashpot system with deadzone are connected by a rigid bar. The input to the multiplay system is the position u of the bar. Each element is modeled by the differential equation

$$\begin{aligned} m_i\ddot{x}_i(t)+c_i\dot{x}_i(t)+k_i d_{2\Delta_i}\big(x_i(t)-u(t)\big)=0,\\ x_i(0)=x_{i0}, \quad t\geq 0, \quad i=1,\dots,N, \end{aligned} \tag{3}$$

where $d_{2\Delta_i}(\cdot)$ is the deadzone function defined by (2). The output of the system is defined as

$$y(t)=\sum_{i=1}^{N} k_i(u(t)-x_i(t)). \tag{4}$$

Physically, $y(t)$ represents the sum of spring forces in the multiplay system. We allow the stiffness coefficients and masses to be negative. We call (3)-(4) the multiplay model, and we omit units since we do not physically construct this system.

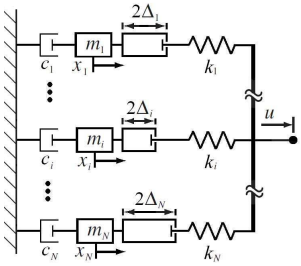

Fig. 3. A schematic representation of the multiplay system consisting of N mass/spring/dashpot with deadzone elements. The elements are connected in parallel by a rigid bar.

The input-output maps of the multiplay model converge to a hysteretic map as the frequency of the periodic input approaches zero as shown in Fig. 4. This figure shows the input-output response of a multiplay model with two elements. For simplicity all masses are set to $m_i=1$, all stiffness coefficients to $k_i=1$, all damping coefficients to $c_i=1$, and the deadzone widths to $\Delta_1=0.8$ and $\Delta_2=0.2$. Furthermore, the multiplay model in Fig. 4 has nonlocal memory. When the direction of the input is reversed after either a half or a full period, the output converges to two distinct trajectories.

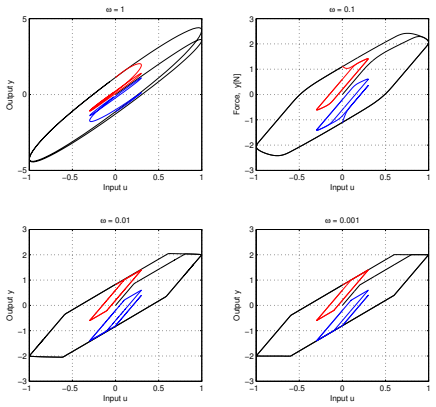

Fig. 4. Periodic input-output maps of the multiplay model. As the frequency of the input approaches zero the periodic input-output map approaches a hysteretic map with nonlocal memory. This hysteretic system is rate dependent.

III. MULTIPLAY AND MAXWELL-SLIP MODEL

In this section we explore the relationship between the multiplay model and the Maxwell-slip model. We begin by taking the time derivative of (3)

$$m_i\dddot{x}_i(t)+c_i\ddot{x}_i(t)=k_i d'_{2\Delta_i}\big(u(t)-x_i(t)\big)\big(\dot{u}(t)-\dot{x}_i(t)\big). \tag{5}$$

In the limit, as the period of the input approaches infinity, the dynamics in (3) become negligible. The effective mass and damping coefficient are zero, and (5) becomes

$$d'_{2\Delta_i}\big(u(t)-x_i(t)\big)\big(\dot{u}(t)-\dot{x}_i(t)\big)=0, \tag{6}$$

which means that either

$$\dot{x}_i(t)=\dot{u}(t) \tag{7}$$

or

$$d'_{2\Delta_i}\big(u(t)-x_i(t)\big)=0. \tag{8}$$

Note that the derivative of the deadzone function exists for all v except $v=-\Delta_i$ and $v=\Delta_i$. Defining the derivative to be 1 at these two points for convenience, we have

$$d'_{2\Delta_i}(v)=\begin{cases} 1, & v\leq -\Delta_i,\\ 0, & |v|<\Delta_i,\\ 1, & v\geq \Delta_i, \end{cases} \tag{9}$$

so that (8) holds if and only if

$$|u(t)-x_i(t)|<\Delta_i. \tag{10}$$

If (10) holds, the end of the spring inside the play element is not in contact with either the left or right wall of the play operator. Thus, the position of the mass is not changing since the end of the spring is neither pushing nor pulling on the

play operator. In other words, $|u(t)-x_i(t)|<\Delta_i$ corresponds to $\dot{x}_i(t)=0$. Now, (7) corresponds to $u(t)-x_i(t)\le-\Delta_i$ and $u(t)-x_i(t)\ge\Delta$. If $u(t)-x_i(t)\le-\Delta_i$ the left end of the spring is pushing on the left wall of the play operator and $u(t)$ is decreasing. If $u(t)-x_i(t)\ge\Delta_i$ the left end of the spring is pushing on the right wall of the play operator and $u(t)$ is increasing. Based on this discussion, in the limit, as the period of the input approaches infinity (3) is equivalent to

$$\dot{x}_i(t)=\begin{cases}\dot{u}(t), & u(t)-x_i(t)\le-\Delta_i, \quad \dot{u}(t)<0,\\ 0, & |u(t)-x_i(t)|<\Delta_i,\\ \dot{u}(t), & u(t)-x_i(t)\ge\Delta_i, \quad \dot{u}(t)>0.\end{cases} \tag{11}$$

Expression (11) can be rewritten as

$$\dot{x}_i(t)=[U(u(t)-x_i(t)-\Delta_i) \quad 1-U(u(t)-x_i(t)+\Delta_i)]\begin{bmatrix}\dot{u}_+(t)\\ \dot{u}_-(t)\end{bmatrix}, \tag{12}$$

$$y(t)=\sum_{i=1}^{N}k_i(u(t)-x_i(t)), \tag{13}$$

where $U(v)$ is the unit step function

$$U(v)\triangleq\begin{cases}1, & v\ge0,\\ 0, & v<0,\end{cases} \tag{14}$$

and $\dot{u}_+(t)$ and $\dot{u}_-(t)$ are defined as

$$\dot{u}_+(t)\triangleq\max\{0,\dot{u}(t)\}, \quad \dot{u}_-(t)\triangleq\min\{0,\dot{u}(t)\}. \tag{15}$$

Equation (12) is a rate-independent semilinear Duhem model of friction, known as the Maxwell-slip model. Thus, in the limit of DC operation, as the frequency of the input approaches zero, the multiplay model (3)-(4) is equivalent to the rate-independent Maxwell-slip model (12)-(13).

IV. DETERMINING THE HYSTERESIS MAP FROM THE MULTIPLAY MODEL

In this section we analyze the properties of the limiting input-output map, that is, the input-output map in the limit as the period of the input approaches infinity.

To find the slope of the limiting input-output map, we differentiate (4) with respect to the input $u(t)$, that is,

$$\frac{dy}{du}=\sum_{i=1}^{n}k_i(1-\frac{dx_i}{du}), \tag{16}$$

where $\frac{dx_i}{du}$ depends on whether m_i is moving or not. Rewriting $\dot{x}_i(t)$ as

$$\frac{dx_i}{dt}=\frac{dx_i}{du}\frac{du}{dt}=\frac{dx_i}{du}\dot{u} \tag{17}$$

and using (11), we have

$$\frac{dx_i}{du}\dot{u}=\begin{cases}\dot{u}(t), & u(t)-x_i(t)\le-\Delta_i, \quad \dot{u}(t)<0,\\ 0, & |u(t)-x_i(t)|<\Delta_i,\\ \dot{u}(t), & u(t)-x_i(t)\ge\Delta_i, \quad \dot{u}(t)>0.\end{cases} \tag{18}$$

From (18) we conclude that

$$\frac{dx_i}{du}=\begin{cases}1, & |u(t)-x_i(t)|\ge\Delta_i,\\ 0, & |u(t)-x_i(t)|<\Delta_i.\end{cases} \tag{19}$$

Substituting (19) into (16) and assuming that, for $i=1,\dots,r$, $|u(t)-x_i(t)|\ge\Delta_i$ and, for $i=r+1,\dots,N$, $|u(t)-x_i(t)|<\Delta_i$, then

$$\begin{aligned}\frac{dy}{du}&=\sum_{i=1}^{r}k_i(1-\frac{dx_i}{du})+\sum_{i=r+1}^{N}k_i(1-\frac{dx_i}{du})\\ &=\sum_{i=1}^{r}k_i(1-1)+\sum_{i=r+1}^{N}k_i(1-0)=\sum_{i=r+1}^{N}k_i.\end{aligned} \tag{20}$$

Once mass m_j starts moving, its stiffness is no longer included in the summation in (20), and thus does not affect the slope of the limiting input-output map until the input u reverses direction and moves $2\Delta_j$ in the opposite direction. The slope of the limiting input-output curve changes each time a stationary mass starts moving. Assuming that the input is oscillating between $u_{\min}$ and $u_{\max}>u_{\min}+2\Delta_N$, if u just reached $u_{\min}$ and is monotonically increasing, none of the masses of the multiplay are moving. The slope of the limiting input-output map, which is equal to the sum of all of the stiffnesses, first changes when u reaches $u_{\min}+2\Delta_1$. The slope becomes the sum of stiffnesses k_2 through k_N. Next, when u increases past $u_{\min}+2\Delta_2$ the slope is equal to the sum of stiffnesses k_3 through k_N. In general, each time u becomes larger then $u_{\min}+2\Delta_i$ the slope decreases by k_i. As the input increases from $u_{\min}$ to $u_{\max}$ the slope changes according to

$$\begin{bmatrix}s_1\\ s_2\\ \vdots\\ s_N\end{bmatrix}=A\begin{bmatrix}k_1\\ k_2\\ \vdots\\ k_N\end{bmatrix} \tag{21}$$

where s_1 is the slope of the section of the hysteresis map that corresponds to $u\in[u_{\min},u_{\min}+2\Delta_1]$ and s_i is the slope of the section of the hysteresis map that corresponds to $u\in[u_{\min}+2\Delta_{i-1},u_{\min}+2\Delta_i]$, $i=2,\dots,N$, and $A\in\mathbb{R}^{N\times N}$ is given by

$$A=\begin{bmatrix}1 & 1 & \cdots & 1\\ 0 & 1 & \cdots & 1\\ \vdots & \vdots & \ddots & \vdots\\ 0 & 0 & \cdots & 1\end{bmatrix}. \tag{22}$$

We demonstrate (20) based on the limiting input-output map of the two-element multiplay shown in Fig. 5(a). The stiffnesses are $k_1=2$ and $k_2=4$, the deadzone widths are $\Delta_1=1$ and $\Delta_2=3$, and $u_{\min}=-5$ and $u_{\max}=5$. In the limit of DC operation, the mass and damping coefficient are irrelevant, and we thus set them equal to the corresponding stiffnesses. The transient response is shown by the dashed line. As the arrows indicate, the hysteresis loop is counter-clockwise. As u increases from $u_{\min}=-5$ to $u_{\min}+2\Delta_1=-3$ the slope of the input-output map is $s_1=6=k_1+k_2$. At this point, the first mass starts moving and the slope becomes

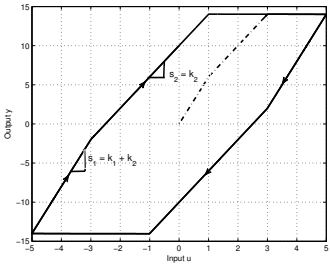

(a)

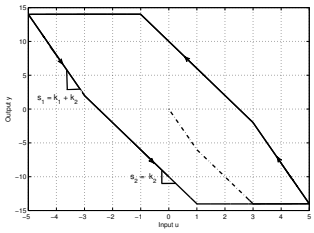

(b)

Fig. 5. Hysteresis map of the multiplay model with two elements and a) positive and b) negative stiffness coefficients. The slope of the hysteresis map at each point is equal to the sum of the stiffness coefficients corresponding to the stationary masses.

$s_2 = 4 = k_2$. When u increases above $u_{\min} + 2\Delta_2 = 1$, the second mass moves and the slope becomes zero. When u reaches $u_{\max}$ and starts decreasing, the slope follows the same rules; in particular the slope is initially 6, then 4, then 0.

The stiffness coefficients k_i do not have to be limited to positive numbers, which allows, the slope of the hysteresis map to be negative. However, if any of the stiffnesses are negative, the corresponding mass and damping coefficient must also be negative in order for system (3)-(4) to be stable. We demonstrate this with the two-element multiplay in Fig. 5(b). The stiffness coefficients are $k_1 = -2$ and $k_2 = -4$. Masses and damping coefficients are equal to the corresponding stiffnesses. All other parameters are the same as in the previous example. The hysteresis map is now counterclockwise, and as u increases from $u_{\min} = -5$ to $u_{\max} = 5$ the slope changes from $s_1 = -6 = k_1 + k_2$, to $s_2 = -4 = k_2$, to $s_3 = 0$.

Positive and negative stiffness coefficients can be combined in the same multiplay model to give S-shaped loops as shown in Fig. 6. The stiffness coefficients are $k_1 = \cdots = k_5 = -1$ and $k_6 = \cdots = k_{10} = 2$. Masses and damping coefficients are equal to corresponding stiffnesses. Deadzone widths are $\Delta = \begin{bmatrix} 1 & 3 & 5 & 7 & 9 & 11 & 13 & 15 & 17 & 19 \end{bmatrix}'$, where the i-th entry of Δ is Δ_i.

V. DETERMINING THE MULTIPLAY MODEL FROM THE HYSTERESIS MAP

Multiplay model can be used to approximate a known hysteresis map that is symmetric under a 180° rotation in the input-output plane, that is, having the symmetry of the cyclic rotational group C_2. The hysteresis map is approximated

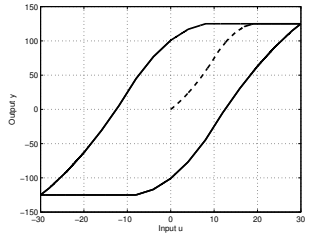

Fig. 6. S-shaped hysteresis map of a multiplay model with ten elements. The S-shape is the result of a combination of positive and negative stiffness coefficients.

by using positive and negative stiffness coefficients to give the desired slope. We divide the hysteresis map into $N+1$ piecewise linear segments, each with slope s_i. Once the slopes are known, the stiffness coefficients can be computed by inverting (21). The matrix A in (21) is nonsingular for all N and its inverse $A^{-1} \in \mathbb{R}^{N\times N}$ is

$$A^{-1} = \begin{bmatrix} 1 & -1 & 0 & \cdots & 0 \\ 0 & 1 & -1 & \cdots & 0 \\ \vdots & \ddots & \ddots & \ddots & \vdots \\ 0 & \cdots & 0 & 1 & -1 \\ 0 & \cdots & \cdots & 0 & 1 \end{bmatrix}. \tag{23}$$

Assuming that the output trajectory from $u_{\min}$ to $u_{\max}$ is partitioned into $N+1$ segments with endpoints $(u_{\min}, y(u_{\min})), (u_1, y(u_1)), \ldots, (u_N, y(u_N)), (u_{\max}, y(u_{\max}))$. The slope of each segment is found from the endpoint coordinates, and the stiffness coefficients are computed from

$$\begin{bmatrix} k_1 \\ \vdots \\ k_N \end{bmatrix} = A^{-1} \begin{bmatrix} s_1 \\ \vdots \\ s_N \end{bmatrix}, \tag{24}$$

where $s_1, \ldots, s_N$ are the slopes of the consecutive segments and the slope s_{N+1} is not used in the calculation. The widths of the deadzones associated with the stiffness coefficients calculated from (24) can be found from

$$\begin{bmatrix} \Delta_1 \\ \vdots \\ \Delta_N \end{bmatrix} = \begin{bmatrix} (u_1 - u_{\min})/2 \\ \vdots \\ (u_N - u_{\min})/2 \end{bmatrix} \tag{25}$$

The following example is taken from [14]. Note that this hysteresis map has the symmetry of the cyclic group C_2. However, the actual data presented in the paper are not available, so the "true" hysteresis map was estimated by "extracting" the points $(u_{\min}, y(u_{\min})), (u_1, y(u_1)), \ldots, (u_N, y(u_N)), (u_{\max}, y(u_{\max}))$ from the plot. Stiffness coefficients and deadzone widths are calculated from (24) and (25), respectively. The estimated and actual hysteresis maps are identical as shown in Fig. 7.

VI. MINOR LOOPS OF THE MULTIPLAY

As already stated, the multiplay system has nonlocal memory, which is manifested as existence of external or

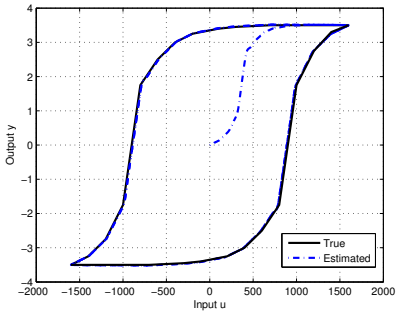

Fig. 7. True and estimated hysteresis maps from [14]. Note that the hysteresis map is symmetric under 180° rotation in the input-output plane, and that the true and estimated hysteresis maps are identical.

internal minor loops that correspond to input reversals.

The shape of the minor loops is determined by the stiffness coefficients k_i and the deadzone widths Δ_i of the masses with Δ_i less than the amplitude of the input reversal. After every input reversal, the initial slope of the reversal loop s_{r1} is given by $s_{r1} = \sum_{i=1}^{N} k_i$.

The slope subsequently changes according to the same rules as described above. When the input reversal occurs at a point of the major loop where the slope of the major loop s_i satisfies $s_i > \sum_{i=1}^{N} k_i$, the minor loop is external. When the reversal happens at the point where the slope of the major loop satisfies $s_i < \sum_{i=1}^{N} k_i$, the minor loop is internal. However, if $s_i = \sum_{i=1}^{N} k_i$, then the minor loop is internal if its slope increases and external if its slope decreases when a stationary mass begins moving.

Minor loops are shown in Figure 8. The figure shows the hysteresis map of a multiplay system and the minor loops that correspond to input reversals at different points along the major loop. The multiplay has 10 masses with stiffness coefficients $k_1 = \cdots = k_4 = -2$ and $k_5 = \cdots = k_{10} = 2$. Masses and damping coefficients are equal to corresponding stiffnesses. Deadzone widths are $\Delta = \begin{bmatrix} 1 & 2 & 4 & 6 & 8 & 10 & 12 & 14 & 16 & 18 \end{bmatrix}'$, where the i-th entry of Δ is Δ_i.

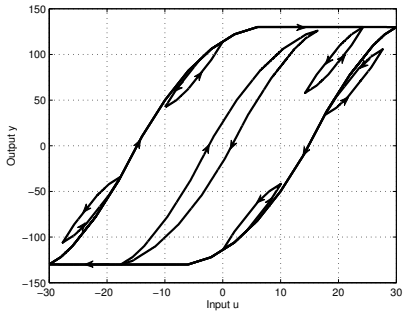

Fig. 8. Internal and external minor loops of an S-shaped multiplay hysteresis map. The major and the large minor loop are clockwise while the small minor loops are counterclockwise.

VII. INVERSE OF THE MULTIPLAY MODEL

In this section we develop the strategy for computing the inverse of a multiplay model with a known hysteresis map. The slopes s_i' of the inverse hysteresis map are

$$s_i' = \frac{1}{s_i}, \quad s_i \neq 0, \tag{26}$$

where s_i is defined in (24). The stiffness coefficients k_i' of the inverse hysteresis map are calculated from s_i' as in (24)

$$\begin{bmatrix} k_1' \\ \vdots \\ k_N' \end{bmatrix} = A^{-1} \begin{bmatrix} s_1' \\ \vdots \\ s_N' \end{bmatrix}. \tag{27}$$

To find the new deadzone widths Δ_i', we use the points $y(u_{\min}), \ldots, y(u_N)$ similarly to (25)

$$\begin{bmatrix} \Delta_1' \\ \vdots \\ \Delta_N' \end{bmatrix} = \begin{bmatrix} (y(u_1) - y(u_{\min}))/2 \\ \vdots \\ (y(u_N) - y(u_{\min}))/2 \end{bmatrix}. \tag{28}$$

One shortcoming of the inverse model obtained through this procedure is that it cannot handle the segments of infinite slope. The inverse hysteresis map of the one in Fig. 6 is shown in Fig 9. Note that the inverse hysteresis maps are counterclockwise. The true and estimated hysteresis map differ only in the vertical segments with infinite slope. However, if the segment of the estimated inverse that corresponds to the decreasing input is shifted up and the segment of the estimated inverse that correspond to the increasing input is shifted down, then the resulting hysteresis map matches the actual inverse hysteresis map.

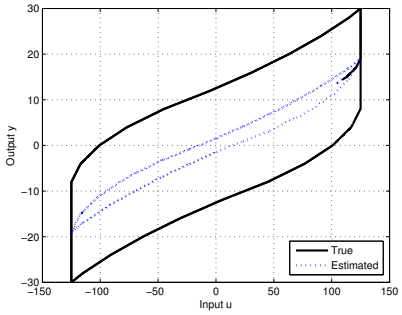

Fig. 9. True and estimated inverse hysteresis maps. Note that the estimated hysteresis map defers from the true only in the vertical segments with infinite slope.

The inverse model obtained from (26)-(28) will give much better results if the original hysteresis map has no zero-slope segments. Figure 10(a) shows a hysteresis map of a multiplay with 10 masses. The stiffness coefficients are $k_1 = \cdots = k_5 = -1$ and $k_6 = \cdots = k_{10} = 2$. Masses and damping coefficients are equal to corresponding stiffnesses. Deadzone widths are $\Delta = \begin{bmatrix} 1 & 3 & 5 & 7 & 9 & 11 & 13 & 15 & 17 & 19 \end{bmatrix}'$, where the i-th entry of Δ is Δ_i. The true and estimated inverses of this hysteresis map are shown in Fig. 10(b). The true and

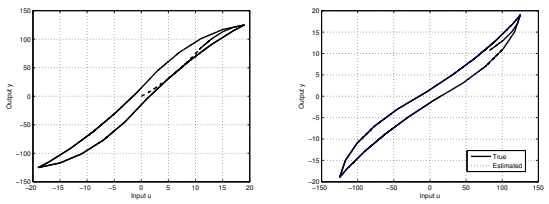

(a) (b)

Fig. 10. Inversion of a hysteresis map without segments having zero slope. The true hysteresis map is shown in a), while its true and estimated inverse is shown in b).

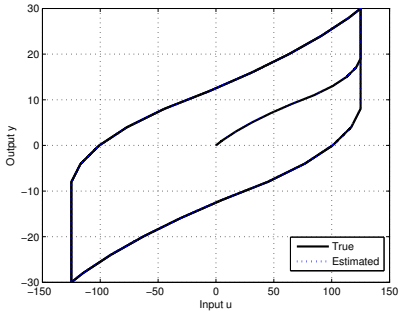

Fig. 11. True and recreated inverse hysteresis maps. The inverse is computed from (31)-(32) based on the known $u(t)$ and $y(t)$.

estimated inverse are now identical.

VIII. ALTERNATIVE INVERSE

In this section we develop an alternative strategy for computing the inverse of any multiplay model given input stiffness coefficients k_i, deadzone widths Δ_i, and the output $y(t)$. If the k_i's and Δ_i's are not given initially, they can be computed through the procedure outlined in Section V. Starting with (4) the input $u(t)$ can be expressed as

$$u(t) = \frac{y(t) + \sum_{j=1}^{N} k_j x_j(t)}{\sum_{j=1}^{N} k_j}, \quad \sum_{j=1}^{N} k_j \neq 0. \tag{29}$$

Substituting (29) into (3) we get

$$m_i \ddot{x}_i(t) + c_i \dot{x}_i(t) + k_i d_{2\Delta_i}\left(x_i - \frac{y + \sum_{j=1}^{N} k_j x_j}{\sum_{j=1}^{N} k_j} \right) = 0. \tag{30}$$

Introducing the change of variables $\bar{u}(t) = y(t)$ and $\bar{y}(t) = u(t)$ in (30) gives a new system

$$\begin{aligned} m_i \ddot{x}_i(t) + c_i \dot{x}_i(t) + k_i d_{2\Delta_i}\left(x_i(t) - \frac{\bar{u}(t) + \sum_{j=1}^{N} k_j x_j(t)}{\sum_{j=1}^{N} k_j} \right) = 0, \\ x_i(0) = x_{i0}, \quad t \geq 0, \quad i = 1, \ldots, N, \quad \sum_{j=1}^{N} k_j \neq 0, \end{aligned} \tag{31}$$

with the output

$$\bar{y}(t) = \frac{\bar{u}(t) + \sum_{j=1}^{N} k_j x_j(t)}{\sum_{j=1}^{N} k_j}, \quad \sum_{j=1}^{N} k_j \neq 0. \tag{32}$$

Fig. 11 shows the inverse of the hysteresis loop displayed in Fig. 6. The output of the multiplay shown in Fig. 6 is used as the input $\bar{u}(t)$ in (31)-(32). Stiffness coefficients, masses, damping coefficients, and deadzone widths remain the same. The actual inverse is also shown for comparison.

IX. CONCLUSIONS

In the present paper we introduced the multiplay model of hysteresis, which consists of a parallel connection of mass/spring/dashpot with deadzone elements. This hysteresis model has nonlocal memory. Multiplay model be used to recreate a known hysteresis map. Parameters of the multiplay model can be determined based on the slope of the desired hysteresis map. We also present an algorithm for inversion of the hysteresis map of the multiplay.

REFERENCES

[1] D. S. Bernstein, "Ivory ghost," *IEEE Contr. Sys. Mag.*, vol. 27, pp. 16–17, 2007.

[2] M. A. Krasnosel'skiĭ and A. V. Pokrovskiĭ, *Systems with Hysteresis*. New York: Springer-Verlag, 1980.

[3] J. Oh and D. S. Bernstein, "Semilinear Duhem model for rate-independent and rate-dependent hysteresis," *IEEE Trans. Autom. Contr.*, vol. 50, no. 5, pp. 631–645, 2005.

[4] A. Visintin, *Differential Models of Hysteresis*. New York: Springer-Verlag, 1994.

[5] A. K. Padthe, B. Drincic, J. Oh, D. D. Rizos, S. D. Fassois, and D. S. Bernstein, "Duhem modeling of friction-induced hysteresis: Experimental determination of gearbox stiction," *IEEE Contr. Sys. Mag.*, vol. 28, pp. 90–107, 2008.

[6] J. Oh, B. Drincic, and D. S. Bernstein, "Nonlinear feedback models of hysteresis: Backlash, bifurcation, and multistability," *IEEE Contr. Sys. Mag.*, vol. 28, pp. 90–107, 2009.

[7] I. D. Mayergoyz, *Mathematical Models of Hysteresis and Their Applications*. Amsterdam: Elsevier, 2003.

[8] M. Brokate and J. Sprekels, *Hysteresis and Phase Transitions*. New York, NY: Springer, 1996.

[9] K. Kuhnen, "Modeling, identification and compensation of complex hysteretic nonlinearities: A modified Prandtl-Ishlinskii approach," *European Jour. of Cont.*, vol. 9, no. 4, pp. 407–418, 2003.

[10] M. A. Janaideh, J. Mao, S. Rakheja, W. Xie, and C. Y. Su, "Generalized Prandtl-Ishlinskii hysteresis model: Hysteresis modeling and its inverse for compensation in smart actuators," *Proc. IEEE Conf. Dec. Contr.*, pp. 5182–5187, 2008.

[11] M. A. Janaideh, S. Rakheja, and C. Y. Su, "A generalized rate dependent play operator for characterizing asymmetric and symmetric hysteresis nonlinearities," *Proc. Amer. Contr. Conf.*, 2008.

[12] F. Al-Bender, W. Symens, J. Swevers, and H. V. Brussel, "Theoretical analysis of the dynamic behavior of hysteresis elements in mechanical systems," *Int. J. Non-Lin. Mech.*, vol. 39, pp. 1721–1735, 2004.

[13] F. Scheibe and M. C. Smith, "A behavioural view of play in mechanical networks," in *Proc. of the European Control Conference*, 2007, pp. 3755–3762.

[14] I. D. Mayergoyz and G. Friedman, "Generalized preisach model of hysteresis," *IEEE Trans. on Magnet.*, vol. 24, no. 1, pp. 212–217, 1988.